JMEPEG (2012) 21:95–100
DOI: 10.1007/s11665-010-9821-z

1059-9495/$19.00

Investigation on Oxygen Chemical Diffusion Properties of Perovskite Oxides $(La_{1-x}Pr_x)_{0.6}Sr_{0.4}Co_{0.8}Fe_{0.2}O_{3-\delta}$

Tiezhu Ding, Luomeng Chao, Wenliang Fan, and Jun Zhang

(Submitted February 22, 2009; in revised form June 25, 2010)

Perovskite oxide samples of $(La_{1-x}Pr_x)_{0.6}Sr_{0.4}Co_{0.8}Fe_{0.2}O_{3-\delta}$ (x = 0.2, 0.4, 0.6, 0.8) are obtained by solid-state reaction method. The oxygen chemical diffusion properties of $(La_{1-x}Pr_x)_{0.6}Sr_{0.4}Co_{0.8}Fe_{0.2}O_{3-\delta}$ are determined by electrical conductivity relaxation technique. The results show that the conductivity of $(La_{1-x}Pr_x)_{0.6}Sr_{0.4}Co_{0.8}Fe_{0.2}O_{3-\delta}$ increases with the increase of oxygen partial pressure. The $(La_{1-x}Pr_x)_{0.6}Sr_{0.4}Co_{0.8}Fe_{0.2}O_{3-\delta}$ samples have a high oxygen chemical diffusion coefficient, which decreases linearly with a decrease in temperature and an increase in Pr content. The oxygen chemical diffusion coefficient D_{chem} remains fairly constant at high PO_2. The oxygen chemical diffusion coefficient is the highest for $(La_{1-x}Pr_x)_{0.6}Sr_{0.4}Co_{0.8}Fe_{0.2}O_{3-\delta}$ with x = 0.2, and attains a value of 9.41×10^{-5} cm^2 s^{-1} at 600 °C. This shows the material's promise as a cathode material for intermediate temperature solid oxide fuel cells.

Keywords advanced characterization, electronic materials, energy

1. Introduction

Doped ABO_3-type perovskites are promising cathode materials for solid oxide fuel cells (SOFC) due to their combined high electronic and ionic conductivities (Ref 1-4). The electronic conductivity and ionic conductivity (oxygen chemical diffusion) are very important parameters when describing the transport properties in mixed conducting oxides. Therefore, the study on how to improve the electronic conductivity and oxygen chemical diffusion coefficient of mixed conducting oxides is quite important (Ref 5-8).

Perovskite rare earth oxides $La_xSr_{1-x}Co_yFe_{1-y}O_{3-\delta}$ (LSCF) are promising candidate materials for solid oxide fuel cells but their conductivity still cannot entirely meet the demands at intermediate temperatures. In this article, doping of lanthanum ion and praseodymium ion in LSCF's A-site for changing average A-site ion radius is attempted to improve the electronic conductivity and oxygen chemical diffusion coefficient of perovskite oxides. $(La_{1-x}Pr_x)_ySr_{1-y}Co_zFe_{1-z}O_{3-\delta}$ (LPSCF) samples are prepared by solid state-reaction method, and the oxygen chemical diffusion coefficient and total electrical conductivities of LPSCF are determined by electrical conductivity relaxation technique and the van der Pauw method. It is found that the LPSCF systems have high oxygen chemical diffusion coefficient, which can be promising cathodes materials for intermediate temperature solid oxide fuel cells.

Tiezhu Ding, Luomeng Chao, and **Wenliang Fan**, School of Physical Science and Technology, Inner Mongolia University, Hohhot 010021, China; and **Jun Zhang**, School of Chemistry and Chemical Engineering, Inner Mongolia University, Hohhot 010021, China. Contact e-mail: clm120@126.com.

2. Theory of Oxygen Chemical Diffusion Coefficient Measurement

Electrical conductivity relaxation technique is the measurement of the time variation of the electrical conductivity of a sample after a stepwise change in the ambient oxygen partial pressure. For the oxides, the sample responds to this change by an uptake or release of oxygen, i.e., changing its oxygen content, and through that, changing its mass and electrical conductivity.

For one-dimensional diffusion in a flat sample with thickness of $2L$, it is assumed that the diffusion is controlled by bulk diffusion and the diffusion coefficient is constant. The starting point in the derivation is Fick's second law:

$$\frac{dC}{dt} = D_{chem}\frac{d^2C}{dx^2} \quad \text{(Eq 1)}$$

where C is concentration of diffusing substance, t is diffusion time, and D_{chem} is chemical diffusion coefficient.

The initial and boundary conditions are:

$$C(x,0) = C_0$$

$$\left.\frac{dC}{dx}\right|_{x=0} = 0$$

where C_0 is the initial concentration of oxide ions in the sample. If surface effects are ignored, then the boundary condition can be expressed as

$$C(\pm L,t) = C_\infty$$

where C_∞ is the final concentration of oxide ions in the sample.Then, the solution of Eq 1 is (Ref 9):

$$\frac{C(t)-C_0}{C_\infty - C_0} = 1 - \sum_{n=0}^{\infty}\frac{8}{(2n+1)^2}\times\exp\left[\frac{(2n+1)^2\pi^2 D_{chem}t}{4L^2}\right] \quad \text{(Eq 2)}$$

The relation of the change of apparent conductivity σ_{app} and $C(t)$ is:

$$\frac{C(t)-C_0}{C_\infty-C_0}=\frac{\sigma_{app}(t)-\sigma_{app}(0)}{\sigma_{app}(\infty)-\sigma_{app}(0)} \quad \text{(Eq 3)}$$

This leads to the expression of time change of the apparent conductivity as:

$$\frac{\sigma_{app}(t)-\sigma_{app}(0)}{\sigma_{app}(\infty)-\sigma_{app}(0)}=1-\sum_{n=0}^{\infty}\frac{8}{(2n+1)^2\pi^2}\times\exp\left[-\frac{(2n+1)^2\pi^2D_{chem}t}{4L^2}\right] \quad \text{(Eq 4)}$$

Assuming that $f(t)=\frac{\sigma_{app}(t)-\sigma_{app}(0)}{\sigma_{app}(\infty)-\sigma_{app}(0)}$ and then

$$1-f(t)=\sum_{n=0}^{\infty}\frac{8}{(2n+1)^2\pi^2}\times\exp\left[-\frac{(2n+1)^2\pi^2D_{chem}t}{4L^2}\right] \quad \text{(Eq 5)}$$

Least-squares fitting of time variation of the $\ln[1-f(t)]$ to Eq 5 allows us to determine the chemical diffusion coefficient D_{chem}.

3. Experimental

3.1 Sample Preparation

The samples of nominal compositions $(La_{1-x}Pr_x)_{0.6}Sr_{0.4}Co_{0.8}Fe_{0.2}O_{3-\delta}$ (x = 0.2, 0.4, 0.6, and 0.8) were prepared by solid state-reaction in air between La_2O_3(99.99%, dried at 550 °C for 5 h), Pr_6O_{11}(99.95%, dried at 550 °C for 5 h), $SrCO_3$ (99.5%), Fe_2O_3(99.8%), and Co_2O_3 (98.5%). After calcination at 1100 °C for 2 h the powders were pressed at 200 MPa with 10 mm in diameter and 2 mm in thickness. Sintering is conducted for 5 h at 1300 °C in air.

3.2 XRD Testing

The perovskite structures is analyzed by the x-ray powder diffraction (Germany BRUKER, D8-ADVANCE) using CuKα radiation (λ = 0.154187 nm, voltage: 40.0 kV, current: 50 mA, scanning rate: 10° min^{-1}, scanning range 2θ: (20° to 80°).

3.3 Oxygen Chemical Diffusion Coefficient Testing

The oxygen chemical diffusion coefficient at 500 to 800 °C is measured by electrical conductivity relaxation method. The conductivity relaxation measurements are carried out by using the Mass Flow controller (D07-7A/ZM, Beijing, China). The samples were mounted in a furnace. Step changes in PO_2 were achieved using two separate nitrogen-diluted oxygen gas flows. Relative changes in the electrical conductivity with a step change in PO_2 were measured with a four-point technique using gold electrodes. The flush time is just about 5 s.

The number of experimental samples is listed in Table 1.

Table 1 Number of samples

Samples	Number
$(La_{0.2}Pr_{0.8})_{0.6}Sr_{0.4}Co_{0.8}Fe_{0.2}O_3$	LPSCF-28
$(La_{0.4}Pr_{0.6})_{0.6}Sr_{0.4}Co_{0.8}Fe_{0.2}O_3$	LPSCF-46
$(La_{0.6}Pr_{0.4})_{0.6}Sr_{0.4}Co_{0.8}Fe_{0.2}O_3$	LPSCF-64
$(La_{0.8}Pr_{0.2})_{0.6}Sr_{0.4}Co_{0.8}Fe_{0.2}O_3$	LPSCF-82

4. Result and Discussion

4.1 Analysis of XRD

Figure 1 shows the room temperature XRD diffraction patterns of $(La_{1-x}Pr_x)_{0.6}Sr_{0.4}Co_{0.8}Fe_{0.2}O_{3-\delta}$ (x = 0.2,0.4,0.6, 0.8) sintered at 1300 °C. It is discernible from Fig. 1 that dominant phase structure of LPSCF systems is perovskite structure. The peaks at 41° and 59° 2θ both consist of two parts. From the literature, $Pr_{0.6}Sr_{0.4}Co_{0.8}Fe_{0.2}O_3$ should form an orthorhombic phase, so we estimate that the left hand peak belongs to rhombohedra phase of $La_{0.6}Sr_{0.4}Co_{0.8}Fe_{0.2}O_3$, and the right-hand peak belongs to orthorhombic phase of $Pr_{0.6}Sr_{0.4}Co_{0.8}Fe_{0.2}O_3$. The right-hand peak becomes increasingly obvious with increasing Pr content. This shows that component of orthorhombic phase is increasing. The peak at 32° 2θ also increases with an increase in Pr content. It is found by analysis that this peak belongs to Pr_2O_3. The appearance of Pr_2O_3 might be attributed to the effect of sintering temperature and time; Optimization of sintering temperature and time shall require further research. The substitution of La^{3+} by Pr^{3+} with a smaller radius leads to decrement of the average A-site cation radius and distorts the original crystalloid structure. The crystallite size of $(La_{1-x}Pr_x)_{0.6}Sr_{0.4}Co_{0.8}Fe_{0.2}O_{3-\delta}$ with x = 0.2, 0.4, 0.6, and 0.8 are 0.09543, 0.09537, 0.09512, 0.09499 nm, respectively.

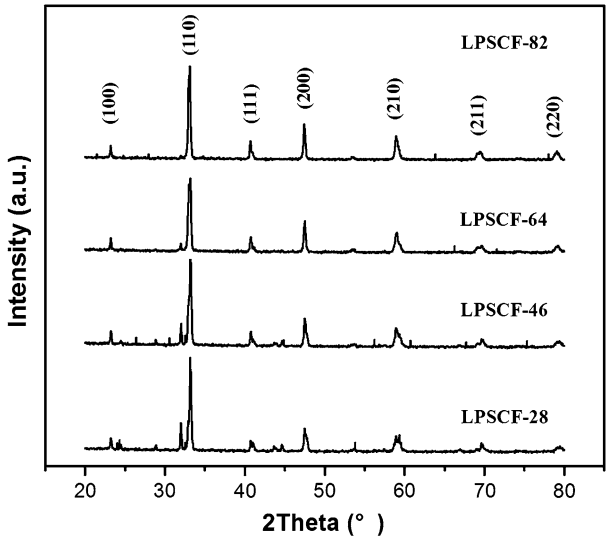

Fig. 1 XRD Pattern of LPSCF samples sintered at 1300 °C for 5 h

4.2 Analysis of Total Electrical Conductivity

Figure 2 shows the total electrical conductivity of LPSCF at 700 °C as a function of oxygen partial pressure. As expected, there is a good linear relationship between $lg(\sigma)$ and $lg(PO_2)$ of LPSCF samples, and the electrical conductivity increases with the increase of oxygen partial pressure, namely $lg(\sigma)$ P n$lg(PO_2)$, where n is constant. It makes clear that the overall reaction can be written as

$$V_o^{\bullet\bullet}+1/2O_2(g)=O_o^X+2h^{\bullet} \quad \text{(Eq 6)}$$

As the PO_2 is increased, the equilibrium reaction moves toward the right in Eq 6 and the concentration of vacancies is reduced thereby increasing the number of electronic charge carriers. As a result, the conductivity increases with the increase of oxygen partial pressure.

It can be obtained from data fitting in Fig. 2 that the electrical conductivities of samples with x = 0.2, 0.4, 0.6, 0.8 exhibit direct proportion with $PO_2^{0.062}$, $PO_2^{0.052}$, $PO_2^{0.037}$, $PO_2^{0.029}$, respectively. The exponent is somewhat smaller, and the change with oxygen partial pressure is slow. The electrical conductivity of LPSCF-82 changes faster than that of other samples with oxygen partial pressure.

Figure 3 shows the electrical conductivity as a function of oxygen partial pressure for LPSCF-82 sample at different temperatures. It can be obtained from the fitting of data from Fig. 3 that the electrical conductivity of sample at 500, 600, 700, 800 °C are in proportion with $PO_2^{0.020}$, $PO_2^{0.044}$, $PO_2^{0.062}$, $PO_2^{0.084}$ respectively. The PO_2 dependence is more distinct at higher temperature. This property of LPSCF samples is similar to that of $La_{0.4}Sr_{0.6}CoO_{3-\delta}$ (Ref 5).

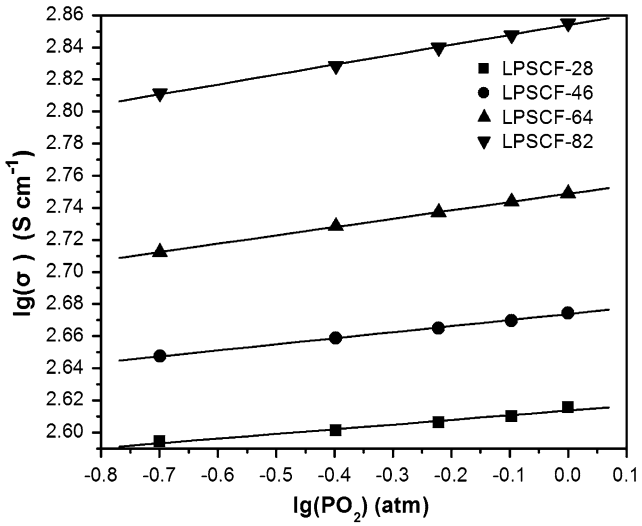

Fig. 2 Total electrical conductivity of LPSCF at 700 °C as a function of oxygen partial pressure

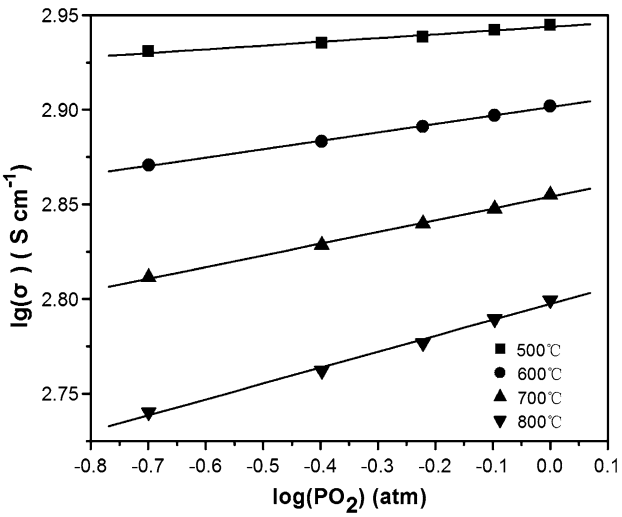

Fig. 3 Total electrical conductivity of LPSCF-82 at different temperatures as a function of the oxygen partial pressure

4.3 Analysis of Oxygen Chemical Diffusion Coefficient

Figure 4 shows the $1-f(t)$ as a function of time for LPSCF samples at 800 °C and Fig. 5 shows the $1-f(t)$ as a function of time for LPSCF-82 sample at different temperatures, with oxygen partial pressure switching from 0.5 to 1.0 atm. It can be seen clearly that the relaxation curves change exponentially, and the measured data are in good agreement with Eq 5.

Least-squares fitting of time variation of the $\ln[1-f(t)]$ in Fig. 4 and 5 allows us to determine the chemical diffusion coefficient D_{chem}. The logarithm of the oxygen diffusion coefficient of LPSCF samples as a function of reciprocal of absolute temperature is shown in Fig. 6. The results show a

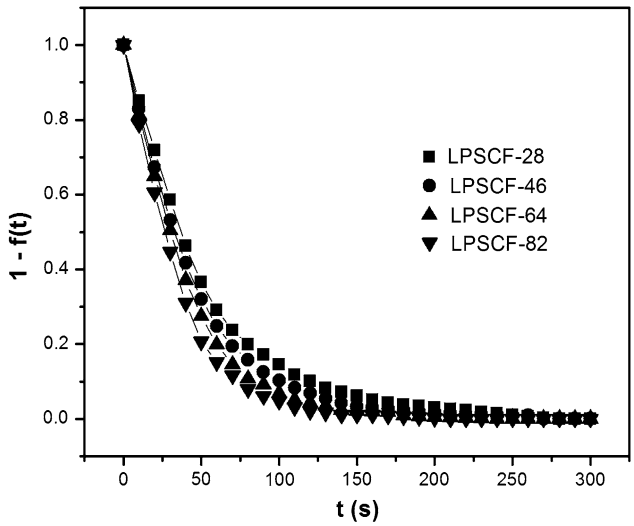

Fig. 4 $1-f(t)$ as a function of time for LPSCF samples at 800 °C with oxygen partial pressure switching from 0.5 to 1.0 atm

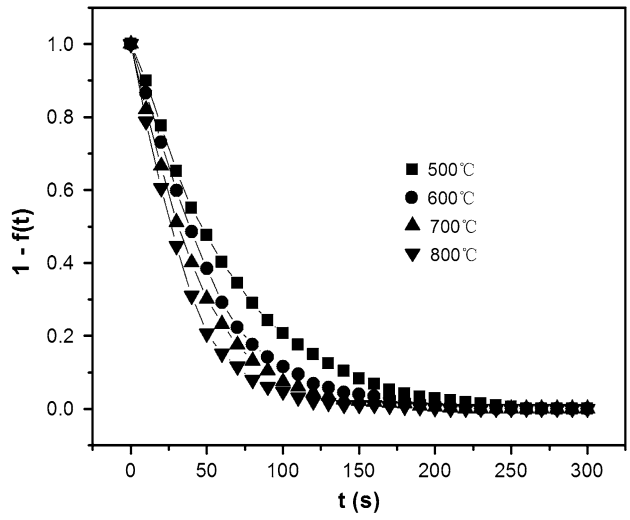

Fig. 5 $1-f(t)$ as a function of time for LPSCF-82 sample at different temperatures with oxygen partial pressure switching from 0.5 to 1.0 atm

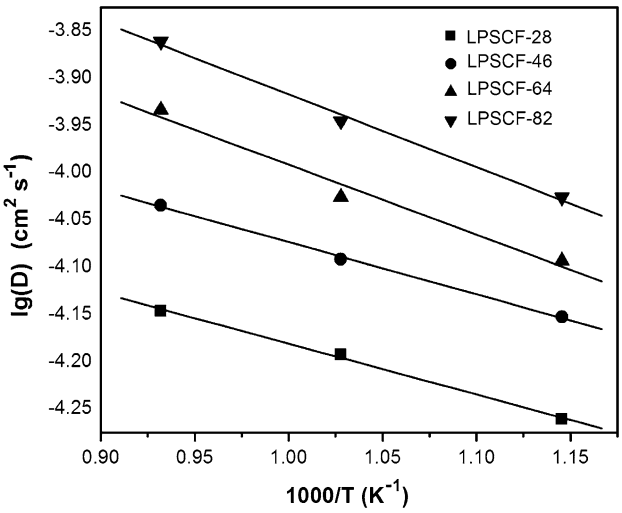

Fig. 6 Logarithm of oxygen chemical diffusion coefficient as a function of reciprocal of temperature for LPSCF

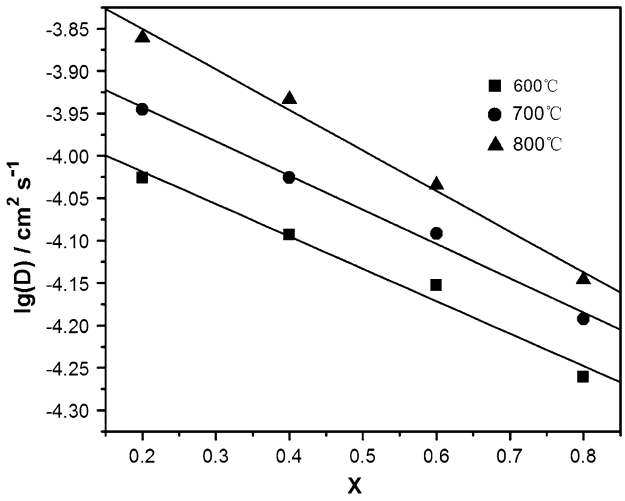

Fig. 7 Logarithm of oxygen chemical diffusion coefficient as a function of Pr content x

linear relationship between lgD_{chem} and the reciprocal of the absolute temperature, lgD_{chem}, reduces with the decrease of temperature. Relationship between D_{chem} and temperature fit Arrhenius relation:

$$D_{chem} = D_0 \exp\left(-\frac{E_a}{K_B T}\right) \quad \text{(Eq 7)}$$

where D_0 is pre-exponential factor, K_B is Boltzmann constant, E_a is activation energy. We can estimate the activation energies of LPSCF-82, LPSCF-64, LPSCF-46, and LPSCF-28 from Fig. 6 by using Least Square Method. The activation energies are about (45.2 ± 1.1), (44.6 ± 2.2), (40.9 ± 0.5), and (40.6 ± 0.6) kJ mol^{-1}, respectively.

The linear relationship between D_{chem} and temperature reflects that the oxygen ion diffusion in perovskite is controlled by heat activation. The increase of temperature provides the energy required for oxygen ions to overcome the bound of ions all around, thus forming more positively charged oxygen vacancies with negatively charged defects. This improves the transfer ability of oxygen ions.

The logarithm of oxygen chemical diffusion coefficient as a function of Pr content x at different temperatures is shown in Fig. 7. The logarithm of oxygen chemical diffusion coefficient decreases with increase of Pr content x at constant temperature. The logarithm of oxygen chemical diffusion coefficient at 600, 700, 800 °C are in proportion with $0.36x$, $0.42x$, $0.46x$, respectively. The content Pr dependence is more distinct at higher temperature.

The oxygen chemical diffusion coefficient of LPSCF samples at 600 °C is listed in Table 2.

It can be seen that the oxygen chemical diffusion coefficient of LPSCF samples is higher than that of $La_{0.6}Sr_{0.4}Co_{0.8}Fe_{0.2}O_{3-\delta}$ reported by Bouwmeester et al. (Ref 10). LPSCF-82 had highest oxygen chemical diffusion coefficient. This might be due to the fact that Pr has better catalytic activity to O atom in perovskite structure than La, and its binding force on O atom is weak. According to Ref 11, LSCFs ionic conductivity is better than PSCFs, while PSCFs catalytic activity is better than LSCFs. Therefore, the ionic conductivity of sample also

Table 2 Oxygen chemical diffusion coefficient of LPSCF samples at 600 °C

Samples	Chemical diffusion coefficient
LPSCF-28	5.48×10^{-5} cm^2 s^{-1}
LPSCF-46	7.03×10^{-5} cm^2 s^{-1}
LPSCF-64	8.07×10^{-5} cm^2 s^{-1}
LPSCF-82	9.41×10^{-5} cm^2 s^{-1}

decreases with an increase in Pr content. But on the other hand, the increase in Pr content leads to the improvement of catalytic activity of samples. We obtained the optimum matching between ionic conductivity and catalytic activity when $x = 0.2$. (we can makes further research on Pr substitution when $x = 0.0$-0.4 in the next step of work). The ionic conductivity decreased with an increase of Pr content. The improvement of catalytic activity cannot compensate the decrease of ionic conductivity, so, the oxygen chemical diffusion coefficient will be decreased.

Figure 8 shows the $1 - f(t)$ as a function of time for LPSCF-64 sample at 700 °C with oxygen partial pressure switching from 1.0 atm to different final oxygen partial pressures. It can be seen that the time to reach equilibrium increases as the oxygen partial pressure is reduced. Also, conductivity relaxation plots are effectively identical for reduction steps if the final PO_2 is the same as illustrated in Fig. 9. There is a good agreement in the result of this experiment with the conclusion reported by others for similar compositions (Ref 6-10, 12-15).

The chemical diffusion coefficient D_{chem} obtained from the fitted data in Fig. 8 has been plotted in Fig. 10 as a function of the final PO_2 in each PO_2 step change. It can be seen that D_{chem} changed little when final oxygen partial pressure changed from 0.5 to 0.8 atm. The general trend is that D_{chem} remains fairly constant at high PO_2. The result from Wang et al. shows that the values of D_{chem} are constant when final $PO_2 > 0.05$ atm for perovskite oxides $La_{0.5}Sr_{0.5}CoO_{3-\delta}$ (Ref 12). Also, Bouwmeester et al. reported that the values of D_{chem} are constant when final $PO_2 > 10^{-2}$ bar for $La_{0.6}Sr_{0.4}Co_{1-y}Fe_yO_{3-\delta}$ (Ref 10), which is consistent with result of this experiment.

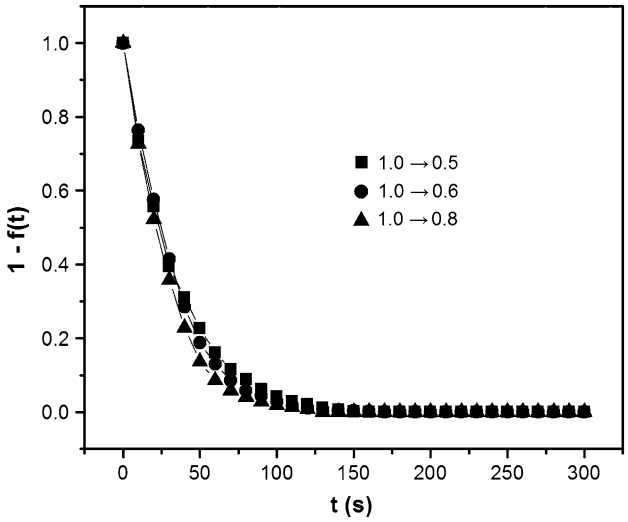

Fig. 8 $1-f(t)$ as a function of time for LPSCF-64 sample at 700 °C for various oxygen partial pressure switches

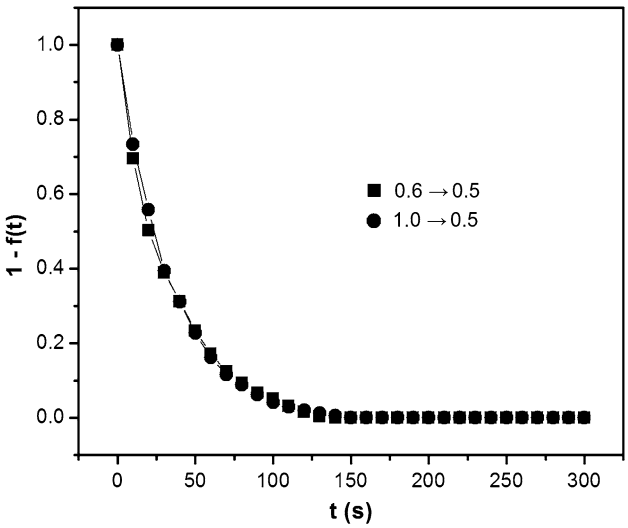

Fig. 9 $1-f(t)$ as a function of time for LPSCF-64 samples at 700 °C with final oxygen partial pressure of 0.5 atm

5. Conclusions

LPSCF samples with x = 0.2, 0.4, 0.6, 0.8 are obtained by solid-state reaction method. The dominant phase structures of LPSCF systems are perovskite structures and multiple phases appear with an increase in Pr content. The electrical conductivity of LPSCF samples increases with the increase of oxygen partial pressure. LPSCF systems have a high oxygen chemical diffusion coefficient, which decrease with a decrease in temperature and an increase in content Pr. The oxygen chemical diffusion coefficient D_{chem} remains fairly constant at high PO_2. In intermediate temperature region (600-800 °C), the oxygen chemical diffusion coefficient of LPSCF systems is higher than 5.48×10^{-5} cm^2 s^{-1}, and the oxygen chemical diffusion coefficient is the highest for the sample with x = 0.2, which attains a value of 9.41×10^{-5} cm^2 s^{-1} at 600 °C. This shows promise as a cathode material for intermediate temperature solid oxide fuel cells.

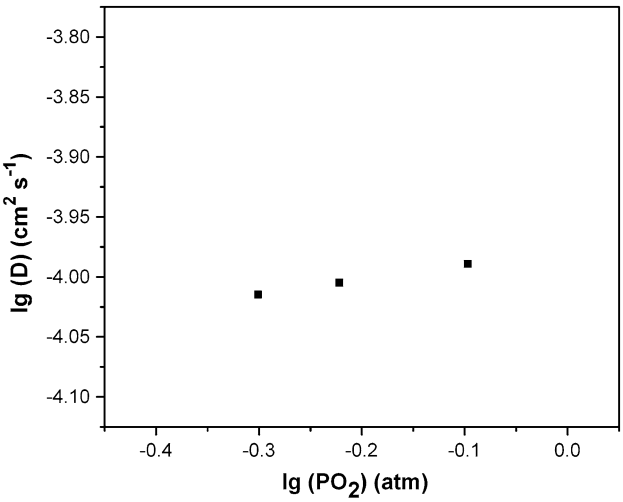

Fig. 10 Chemical diffusion coefficient versus oxygen partial pressure for LPSCF-64

Acknowledgments

This work was supported by the National Natural Science Foundation of China (project No. 10464001) and Key Natural Science Foundation of Education Department of Inner Mongolia (project No. NJ09002).

References

1. A. Petric, P. Huang, and F. Tietz, Evaluation of La-Sr-Co-Fe-O Perovskite for Solid Oxide Fuel Cells and Gas Separation Membranes, *Solide State Ion.*, 2000, **135**, p 719–725
2. M. Mori, Y. Hiei, N.M. Sammes, and G.A. Tompsett, Sinternig Behavior of Ca-or Sr-Doped $LaCrO_3$ Perovskites Including Second Phase of $AECr_{0.4}$(AE = Sr, Ca) in Air, *J. Electrochem. Soc.*, 2000, **147**(4), p 1295–1302
3. T. Ding, J. Li, Q. Qi, B. Ji, J. Liu, and C. Zhang, XPS Studies on Rare Earth Oxide LSCO/YSZ Electrodes, *J. Rare Earths*, 2003, **21**(4), p 453–458
4. T.Z. Ding, Y.M. Wang, and S.H. Shi, Electrical Transport Behavior of Perovskite-Type Oxide LSCO, *Mater. Sci. Lett.*, 2003, **22**(1), p 1–3
5. E. Bucher, W. Jantscher, A. Benisek, W. Sitte, W. Preis, I. Rom, and F. Hofer, Transport Properties of $La_{0.4}$ $Sr_{0.6}$ $CoO_{3-\delta}$, *Solid State Ion.*, 2001, **141–142**, p 375–380
6. I. Yasuda and M. Hishinuma, Chemical Diffusion in Polycrystalline Calcium-Doped Lanthanum Chromites, *J. Solid State Chem.*, 1995, **0115**, p 152–157
7. I. Yasuda and M. Hishinuma, Electrical Conductivity and Chemical Diffusion Coefficient of Sr-Doped Lanthanum Chromites, *Solid State Ion.*, 1995, **80**, p 141–150
8. J.A. Lane, S.J. Benson, D. Waller, and J.A. Kilner, Oxygen Transport in $La_{0.6}Sr_{0.4}Co_{0.2}Fe_{0.8}O_{3-\delta}$, *Solid State Ion.*, 1999, **121**, p 201–208
9. M. Katsuki, S. Wang, K. Yasumoto, and M. Dokiya, The Oxygen Transport in Gd-Doped Ceria, *Solid State Ion.*, 2002, **154–155**, p 589–595
10. H.J.M. Bouwmeester, M.W. Den Otter, and B.A. Boukamp, Oxygen Transport in $La_{0.6}Sr_{0.4}Co_{1-y}Fe_yO_{3-\delta}$, *Solid State Electrochem.*, 2004, **8**, p 599–605
11. T. Ishihara, T. Kudo, H. Matsuda, and Y. Taita, Doped $PrMnO_3$ Perovskite Oxide as a New Cathode of Solid Oxide Fuel Cells for Low Temperature Operation, *J. Electrochem. Soc.*, 1995, **142**, p 1519–1524

12. J.A. Lane and J.A. Kilner, Measuring Oxygen Diffusion and Oxygen Surface Exchange by Conductivity Relaxation, *Solid State Ion.*, 2000, **136–137**, p 997–1001
13. S. Wang, A. Verma, Y.L. Yang, A.J. Jacobson, and Ben Abeles, The Effect of the Magnitude of the Oxygen Partial Pressure Change in Electrical Conductivity Relaxation Measurements: Oxygen Transport Kinetics in $La_{0.5}Sr_{0.5}CoO_{3-\delta}$, *Solid State Ion.*, 2001, **140**, p 125–133
14. T. Ramos and A. Atkinson, Oxygen Diffusion and Surface Exchange in $La_{1-x}Sr_xFe_{0.8}Cr0.2O_{3-\delta}$ (x = 0.2, 0.4 and 0.6), *Solid State Ion.*, 2004, **170**, p 275–286
15. W. Preis, E. Bucher, and W. Sitte, Oxygen Exchange Kinetics of $La_{0.4}Sr_{0.6}FeO_{3-\delta}$ by Simultaneous Application of Conductivity Relaxation and Carrier Gas Coulometry, *Solid State Ion.*, 2004, **175**, p 393–397